Strength of recluse spider's silk originates from nanofibrils

— *Supporting Information* —

*Qijue Wang, Hannes C. Schniepp**

Applied Science Department, The College of William & Mary, P.O. Box 8795, Williamsburg, VA, 23187-8795, USA. E-mail: schniepp@wm.edu

DOI: 10.1021/acsmacrolett.8b00678

1. Materials and methods

1.1 Atomic force microscopy (AFM).

All AFM imaging in Figures 1–4 was carried out in tapping mode using a Ntegra Prima AFM (NT-MDT) along with the Universal head and a 100 μm × 100 μm × 10 μm closed-loop piezo scanner. The AFM was operated in air with controlled relative humidity of 30–50%. AFM probes with a curvature radius about r=8 nm, a resonance frequency f=325 kHz and a nominal spring constant k=40 N/m were used (μmasch, model "HQ: NSC15/Al BS"). AFM scans were square with sizes from 1 μm to 6 μm and pixel resolutions of 1024 × 1024. Gwyddion (http://www.gwyddion.org) was used to flatten topography images. The 3D topography images were rendered using Blender (http://www.blender.org).

1.2 Sample preparation.

The *Loxosceles laeta* spider specimens were kept in individual capsules at ambient conditions (22 °C and 30–50% relative humidity) and were fed with small crickets. The major ampullate (MA) silk threads produced by *Loxosceles* spiders were collected from cotton strips stored in their capsules. A caliper with two needles attached to its jaws was used to remove the threads from the cotton strips to prevent excessive tension in the threads. To prepare the ruptured

silks, threads of *Loxosceles* MA silk were suspended between the two needles of the caliper and extended to failure. To obtain the scratched silks, ribbons were first placed on glass slides and imaged via tapping-mode AFM. A tapping mode AFM probe was then landed on the surface of the ribbon in contact mode, which allowed us to accurately control the applied force on the cantilever to penetrate the surface of the silk. Using the same force set point the AFM probe was then directed away from the silk under constant force conditions to scratch the silk. For preparation of partially dissolved of silk ribbons, *Loxosceles* strands were place between cover glass slips and exposed to hexafluoroisopropanol (HFIP, >99%, MP Biomedicals) for approximately 30 seconds. One cover slip was subsequently removed to allow the sample to dry. AFM imaging was then carried out on the dried samples.

1.3 Scanning electron microscopy (SEM).

SEM images were acquired using a S4700 SEM (Hitachi). For Figure 1d, the silk ribbons were deposited on carbon tape attached to the sample stub and sputter coated with AuPd for 60 seconds to obtain a uniform coating of 2–3 nm thickness. Imaging was carried out at a working distance of 10.7 mm, an acceleration voltage of 5.0 kV and a magnification of 906×. For Figure 3e, the silk ribbons were first deposited on a silicon substrate and scratched by AFM. The substrate was then mounted onto an aluminum stub with silver glue and sputter coated as described above. Working distance for Figure 4a was 6.1 mm, acceleration voltage 5.0 kV and the magnification 25,000×.

1.4 Focused ion beam (FIB).

For focused ion beam (FIB) milling, a silk ribbon was placed on a copper substrate and sputter coated. FIB milling was then carried out using a Helios 600i (FEI) instrument using a Ga^+ ion beam with 5 kV acceleration voltage and an ion current of 41 pA. In-situ SEM imaging using the same instrument was carried out at a 2 kV acceleration voltage, 21 pA electron current, 6 µs dwell time, and 4.2 mm working distance.

1.5 Tensile testing

To prepare the sample for the tensile testing, an adult female *Loxosceles laeta* spider was first anesthetized with a gentle flow of CO_2 and then pinned down on its dorsal side for silk collecting. The silk produced by the spider was collected at a rate of about 1 cm/s with a home-

made mandrel (equipped with equally spaced collecting bars) to prevent any excessive tension being applied to the silk strand. A C-shaped frame made from cardstock paper was brought close to the silk strand between the collecting bars for silk transfer. The ribbon was glued to both sides of the frame and cut from the rest of the silk strand. A Keysight T150 tensile tester was used to perform the tensile test. The C-shaped cardstock frame was first clamped to the arms of the tensile tester, and then its vertical edge was cut to freely suspend the silk ribbon. The tensile test was performed at an extension rate of 1 mm/min.

2. Supporting data

2.1 Nanofibril width measurements

For maximal accuracy in determining fibril widths from atomic force microscopy (AFM) topography data, we chose cross-sections to begin and end in the center of a nanofibril, at maximal height, spanning as many fibrils as possible (typically 3–4 nanofibrils). The measured distances were then divided by the number of fibrils in each cross-section to obtain the average center-to-center spacing between two fibrils. Assuming that the fibrils touch each other, this distance is equivalent to their width and provides an accurate measurement of their width. Averaging over several fibrils reduces uncertainty, and measuring the center position of a fibril is independent of the size of the AFM probe and is thus not affected by tip shape artefacts that typically compromise accurate AFM size measurements of nanoscale objects.

For the silk thread featured in Figure 1e of the main text, a total of 50 surface topography cross-sections were examined to determine the average nanofibril width. Three of the 50 cross-sections are shown in Figure S1 (same AFM image as Figure 1e of the main text). Altogether, we measured 5 threads from 4 different *Loxosceles* specimens (3 females, 1 male). Average nanofibril width from different individual spiders, different sexes and different weight all fell into the range of about 20–24 nm. See Table S1 and Figure S2 for further details and additional atomic force microscopy (AFM) topography images.

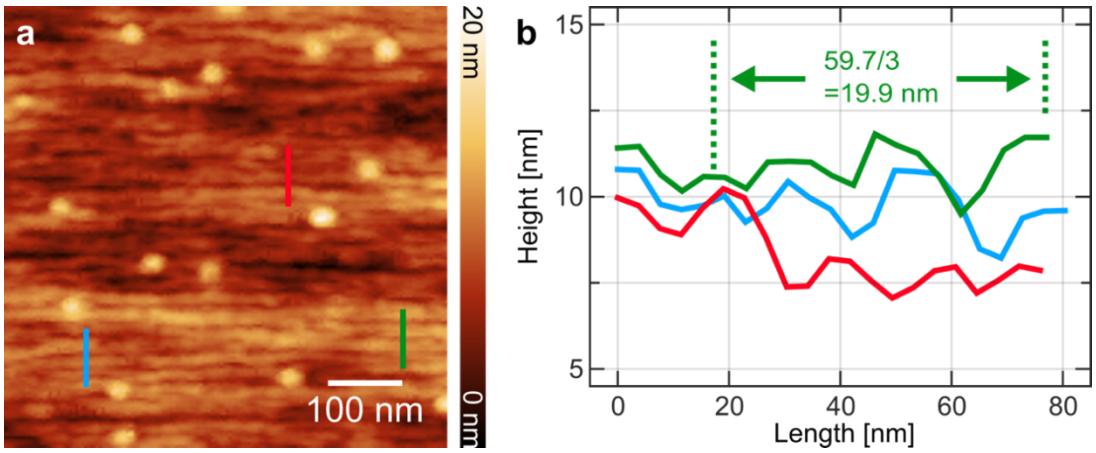

Figure S1. Three of the examined topography cross-sections of nanofibrils on the *Loxosceles* ribbon silk surface. a) Atomic force microscope (AFM) topography image of the silk surface. The same image is featured in Figure 1e of the main text. b) Three cross-sections of the nanofibrils, whose locations are indicated in panel (a) with corresponding colors.

Individual	Sex	Spider Weight (mg)	No. of Locations Measured	Average Width (nm)
A (thread 1)	F	387	50	21.3 ± 3.3
A (thread 2)	F	387	10	23.8 ± 3.3
B	F	205	9	23.1 ± 2.2
C	F	181	9	20.9 ± 1.8
D	M	121	10	20.2 ± 1.9

Table S1. Average nanofibril width from 4 different specimens. Thread 1 from specimen A was used in the main text, Figure 1e.

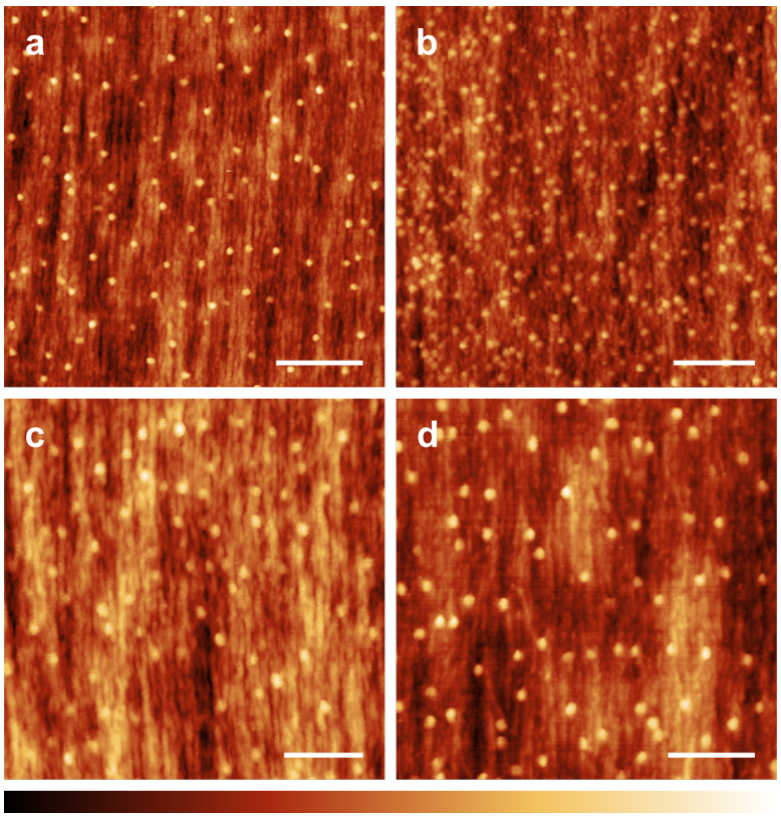

Figure S2. Additional AFM topography images of the surface of different silk strands produced by specimens A (a), B (b), C (c) and D (d). Similar nanofibril widths were observed for all samples. Scale bars: a), b) 300nm, c), d) 200nm. Color bar: a) 0–19 nm, b) 0–20 nm, c) 0–15 nm, d) 0–20 nm.

2.2 Thickness of the fractured silk

Ten topography section profiles were chosen across the fracture edge (positions indicated by colored, dashed lines in Figure S3a, which was featured in Figure 2a of the main text) and used to calculate the thickness of the tested ribbon. The corresponding cross-sections are shown in matching colors in Figure S3b. The measured average thickness was 57.5 ± 4.5 nm.

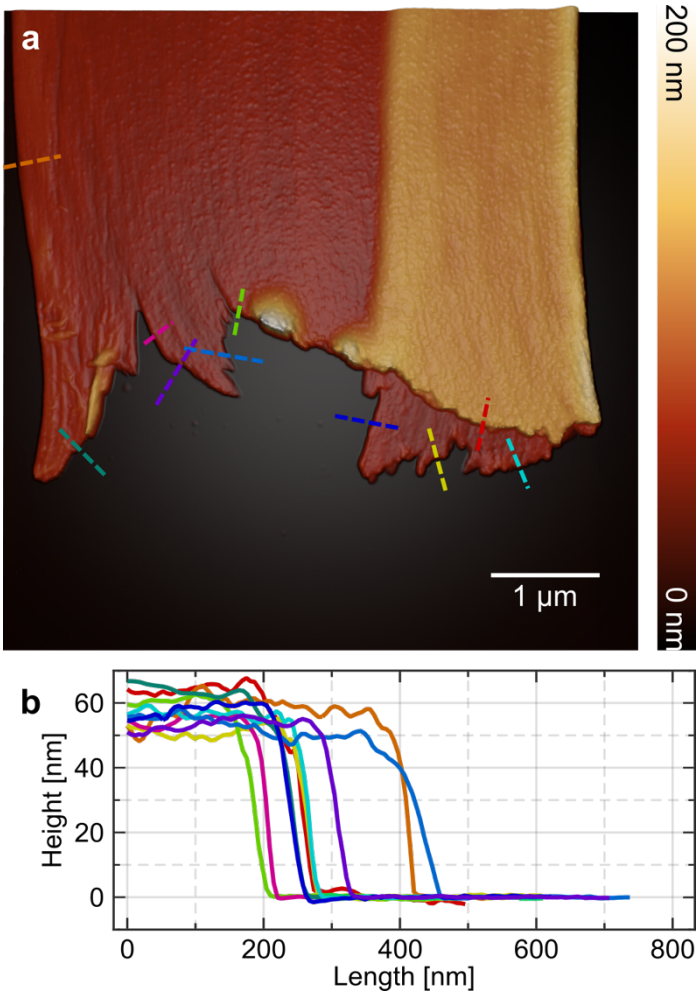

Figure S3. Ten cross-sections chosen to characterize the ribbon thickness. a) Dashed lines with different colors represent the profile locations. b) Cross-sections taken from locations indicated in panel (a) in corresponding colors.

2.3 Stepped topography profiles of the fractured silk

Similarly, five section profiles were chosen in the AFM image featured in Figure S4 (AFM image with lower magnification featured in Figure 2a of the main text) to characterize the step heights across the fracture edge. Dashed lines with different colors in Figure S4a represent the locations of five cross-sections with corresponding colors in Figure S4b.

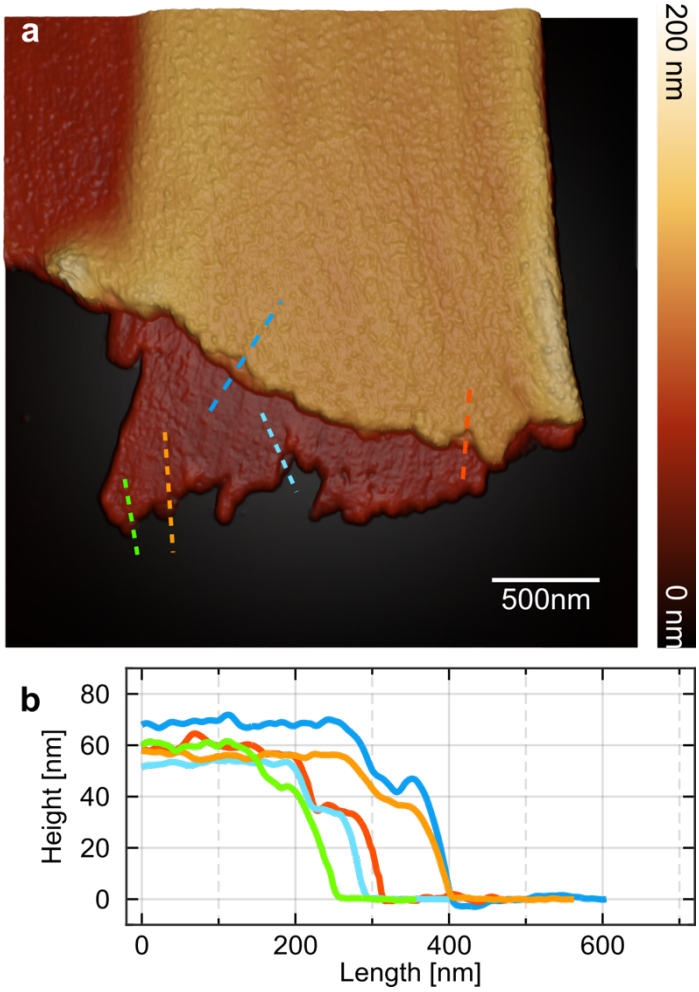

Figure S4. Five cross-sections chosen to characterize the step heights. a) Dashed lines with different colors represent the profile locations. b) Cross-section profiles of the steps observed in the fracture edge of *Loxosceles* ribbon.

2.4 Thickness estimation of the single layer of nanofibrils

Featured in the inset of Figure 2b in the main text, the AFM topography image shown here as Figure S5a exhibits an oval surface defect, at which the topmost layer of nanofibrils appears to be "torn open". We used this defect to estimate the thickness of the topmost layer of nanofibrils via AFM topography; four topography cross-sections featured in Figure S5c (left) were chosen. We also used a single layer of nanofibrils after partial silk ribbon dissolution using hexafluoroisopropanol (HFIP) (Figure S5b) to assess fibril thickness; several locations were investigated (Figure S5c, right). We found the height analysis based on these topography cross-sections quite challenging due to large local height variations; consequently, our estimate yielded a range of 5–9 nm.

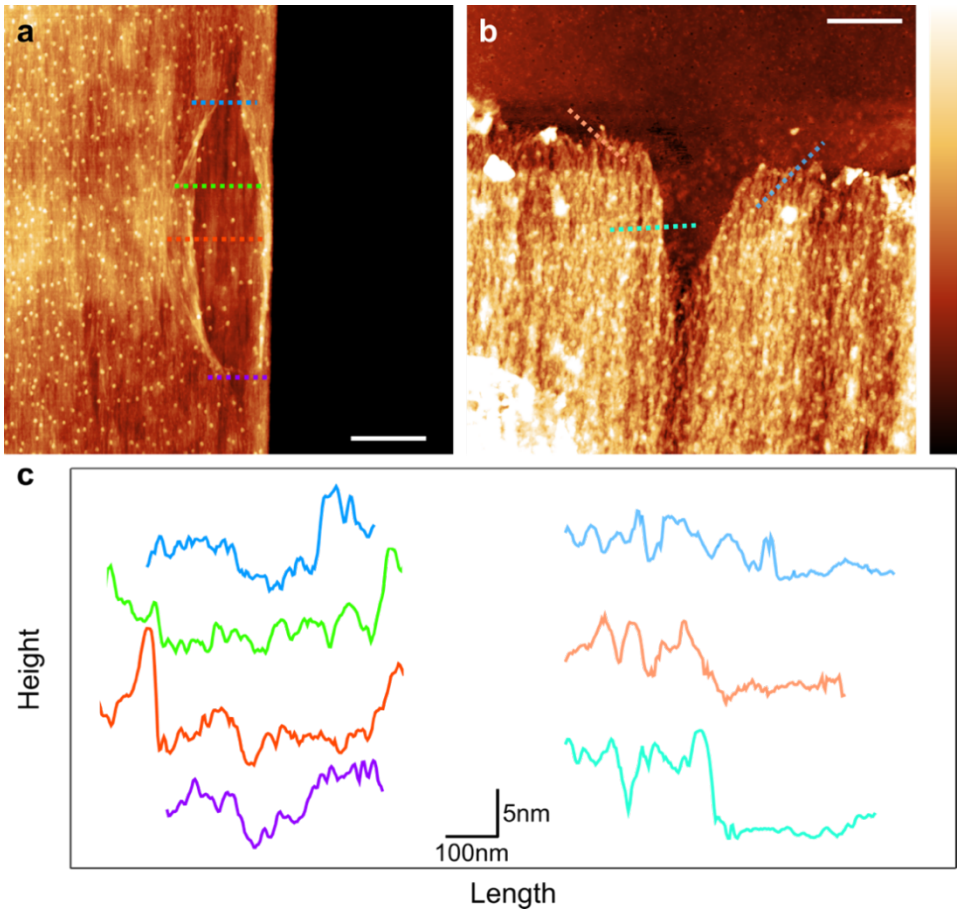

Figure S5. a) AFM topography image featuring a surface defect in the ribbon (tapping mode). The same figure was shown as Figure 2b inset in the main text. b) AFM topography image of a single layer of nanofibrils following the partial dissolution of ribbon silk. c) Cross-sections chosen to estimate the thickness of the nanofibrillar layer. Positions in the images are shown by dashed lines in corresponding colors in a) and b). Scale bars: a, b) 500 nm. Color bar: a) 40–70 nm; b) 0–17 nm.

2.5 Details about AFM-made trench and nanofibril width measurement within

As Figures 3a and 3c of the main text and Figures S6a and S6b show, the debris produced via AFM scratching was predominantly located on one side of the trench. The AFM probes we used feature pyramidal tips, where the base of the pyramid is a kite, thus asymmetric (Figure 3a). The observed location of the debris was in agreement with what one would have expected based on this geometry, the orientation of the probe, and the scratching direction relative to the sample.

To characterize the average nanofibril width within the trench, ten cross-sections were chosen (Figure S6) from the AFM magnitude image of the scratched region. Same center-to-center nanofibril width measurement technique was also employed. Colored lines in Figures S6a and S6b represent the locations of the profiles shown in Figure S6c and S6d in corresponding colors. The measured average nanofibril width was 17.6 ± 1.5 nm.

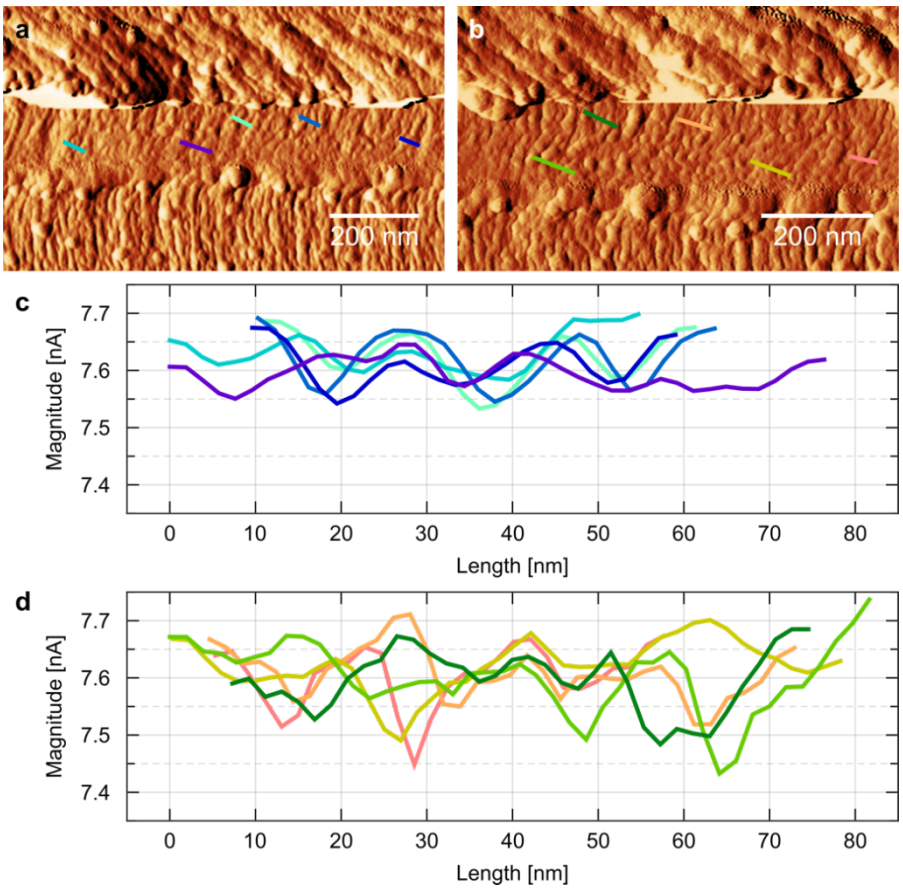

Figure S6. Ten cross-sections chosen to characterize the nanofibril width within the scratched trench. a, b) Solid lines with different colors represent the profiles locations. c, d) Cross-sections of the nanofibril widths observed within the trench. The measured average nanofibril width was 17.6 ± 1.5 nm (n=10).

2.6 Nanofibril length and cross-sectional profiles measurement

Figure S7 shows additional measurements of individual nanofibril length, height and width. For nanofibril length characterization, we characterized one more nanofibril (Figure S7b) in addition to the nanofibril featured in Figure 4d of the main text. This nanofibril was measured to be at least 1.17 μm long. As a guide to the eye, the dashed line in Figure S7b follows the continuous shape of the actual nanofibril.

Additional characterization of nanofibril widths and heights was carried out via AFM topography sections measured on the two individual nanofibrils shown in Figures S7b and S7c. The positions of the cross-sections are indicated by short colored lines in these panels. The actual topography profiles are shown in Figure S7d in corresponding colors. The average width and height for these two nanofibrils were 38.5 nm and 8.2 nm, respectively (n=7).

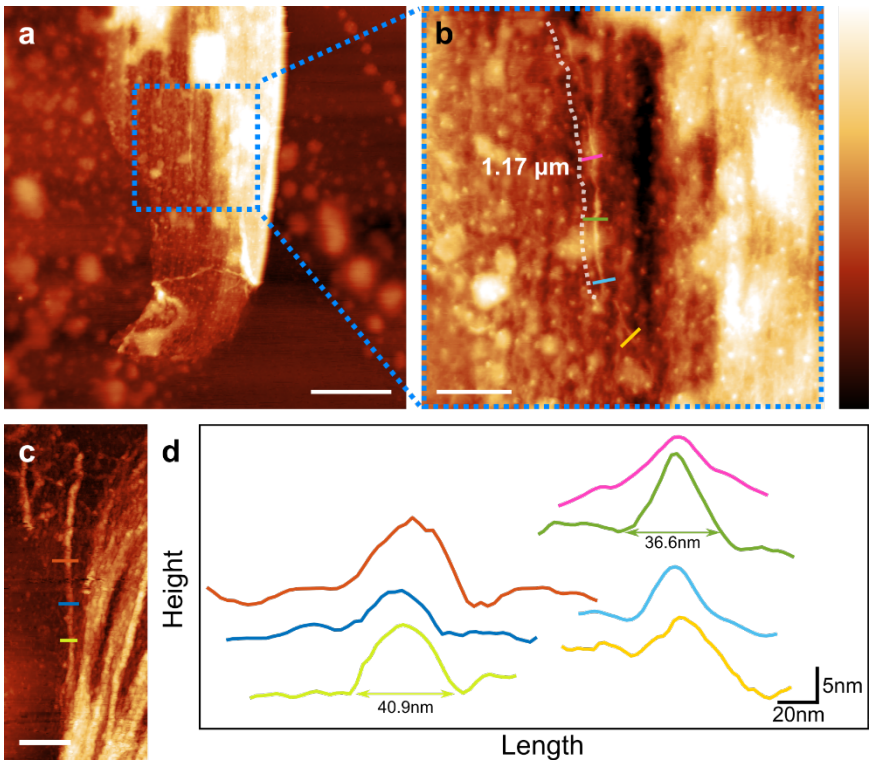

Figure S7. Measurement of individual nanofibril length after partial HFIP dissolution. a) AFM topography image of partially dissolved *Loxosceles* ribbon silk. Several individual nanofibrils can be seen. b) Higher magnification image features one of the individual nanofibrils. c) The nanofibril already featured in Figure 4d of the main text. d) Cross-sectional profiles measured on individual nanofibrils in Figures S7b and S7c, with locations indicated by short lines in matching colors. Scale bars: a) 1 μm; b, c) 300 nm. Color bar: a) 0–65 nm; b) 0–27 nm; c) 0–30 nm.